EUROFUSION WPMST1-PR(16) 14767

F Reimold et al.

The High-field Side High Density Region in SOLPS-Modeling of Nitrogen-seeded H-Modes in ASDEX Upgrade

Preprint of Paper to be submitted for publication in
22nd International Conference on Plasma Surface Interactions in Controlled Fusion Devices (22nd PSI)

This work has been carried out within the framework of the EUROfusion Consortium and has received funding from the Euratom research and training programme 2014-2018 under grant agreement No 633053. The views and opinions expressed herein do not necessarily reflect those of the European Commission.

O15

The High field Side High Density Region in SOLPS-Modeling of Nitrogen-seeded H-Modes in ASDEX Upgrade

F. Reimold[a,*], M. Wischmeier[a], S. Potzel[a], L. Guimarais[1], D. Reiter[b], M. Bernert[a], M. Dunne[a], T. Lunt[a], the ASDEX Upgrade Team[a], the EUROfusion MST1 team[d]

[a]*Max-Planck-Institut für Plasmaphysik, Boltzmannstraße 2, D-85748 Garching,Germany*
[b]*Institut für Energie- und Klimaforschung - Plasmaphysik, Forschungszentrum Jülich GmbH*
[c]*Instituto de Plasmas e Fusão Nuclear, Universidade de Lisboa, Portugal*
[d]*see http://www.euro-fusionscipub.org/mst1*

Abstract

The understanding of divertor physics and the evolution of divertor detachment is crucial for developing the capability to model power exhaust in current experiments and reliably predict it for future fusion devices. Validated modeling with SOLPS5.0 shows that it can be essential to match the details of the high field side scrape-off layer plasma in order to correctly describe the global plasma solution. In simulations of ASDEX Upgrade, an experimentally observed region of high density in the high field side scrape-off layer has been recovered. This high field side high density plays an important role in the fueling of the core plasma and determines the achievable neutral compression in the divertor. Drifts seem to play a crucial role in lower-single null discharges with forward toroidal field ($\nabla\vec{B}$-drift pointing down). Including drifts significantly changes the spatial extent as well as the radial and poloidal gradients of the high field side high density. Adapted diffusive and additional convective radial transport coefficients now reconcile the modeled deuterium compression ratio, divertor neutral density, neutral radiation levels and deuterium fueling rates with experimental measurements. The onset of strong volume recombination in the simulations now allows to remove the previously necessary increase of perpendicular transport in the inner divertor from the simulations.

Keywords: *PACS:* 52.55.Rk, 52.25.Xz, 52.25.Vy, 52.55.Fa
PSI-21: Edge modeling, Divertor plasma, ASDEX-Upgrade, Detachment, High field side high density

*Corresponding author
Email address: f.reimold@fz-juelich.de
(**F. Reimold**)

1. Introduction

Future fusion devices like ITER [1] and DEMO [2] will have to be operated with a detached divertor to meet material limits, which are otherwise largely exceeded at the divertor targets [3, 4]. A sound understanding of the controlling physics in the divertor and scrape-off layer plasma as well as of the interplay of the individual processes in the evolution of divertor detachment is crucial for developing the capability to accurately model power exhaust experiments in current devices such as ASDEX Upgrade or JET [5, 6] and ultimately develop a predictive capability for future fusion devices, such as ITER or DEMO. Previous numerical modeling with SOLPS5.0 has shown that most experimental measurements can be reproduced in the fluctuating and completely detached plasma scenarios in nitrogen-seeded ASDEX Upgrade H-Modes [5, 7]. However, the neutral density and compression in the (sub-)divertor could not be reproduced using the experimental upstream profiles [7]. The persistent discrepancy with experiment manifested in the simulations via an underprediction of the neutral flux densities, the line-integrated Balmer line intensities (D_δ & D_ϵ) and the deuterium fueling rates. In addition, almost no volume recombination occurred in these simulations despite experimental indications of recombining plasma in the inner divertor [8].

This paper presents new SOLPS5.0[1] modeling, which shows that it can be crucial to match the experimental measurements in *both* divertors accurately in order to obtain an improved plasma solution.

It has been shown experimentally that a region of high density in the high field side scrape-off layer – the so-called high field side high density (HFSHD) – is connected to the evolution of the divertor towards complete detachment and to the fueling of the core plasma [9, 10, 5, 11]. Such a high density region also forms in our simulations of the fluctuating detachment state, where it plays an important role in the fueling of the core plasma and determines the achievable neutral pressure in the divertor for a given upstream separatrix density. Consistent with experimental data, the high density region forms with sufficient heating power [10, 12] and extends out of the divertor up to the inner midplane [11]. The nature of the core plasma fueling is changed – with potential implications for plasma performance [12, 13] – and is at least partly responsible for the previous discrepancies of modeling and experiment in the particle throughput and divertor neutral density. An improved match of the high field side scrape-off layer plasma and the detailed analysis of its dynamics enables us to match the experimental neutral compression, fueling rates and to obtain a significant recombination sink for ions in the inner divertor, while maintaining comparable agreement with the other experimental measurements as previous modeling [7].

The experimental setup of the modeled H-mode experiments is shortly presented in Section 2. The modeling setup is detailed in Section 3. The impact of the high field side high density on the simulations and of input parameters on the high field side high density is discussed in Section 4. A discussion and summary in Section 5 closes the paper.

[1] Modified SVN Revision 4551 at http://solps-mdsplus.aug.ipp.mpg.de/repos/SOLPS/trunk/solps5.0/

2. The Experimental Setup

The selected ASDEX Upgrade H-mode discharge (#28903) was a lower single null configuration with a plasma current of $I_\mathrm{P} = 800$ kA, a toroidal field of $B_\mathrm{t} = 2.5$ T ($\nabla\vec{B}$-drift points down) and a total heating power of $P_\mathrm{H} = 8.2$ MW. The separatrix electron density is about $n_\mathrm{e} = 2.5 \times 10^{19}$ m^{-3} with a central line integrated density of $\langle n_\mathrm{e}\rangle = 6.8 \times 10^{19}$ m^{-3}. Measured core plasma impurity concentrations were about $c_\mathrm{N} = 0.5$ %, $c_\mathrm{C} \approx 0.1$ %, $c_\mathrm{He} \approx 0.5$ % in the modeled, non-seeded reference phase. The tungsten core concentration varied between $c_\mathrm{W} = 1.5 - 3.0 \times 10^{-5}$. The discharge #28903 is modeled for a time slice from 2.0 − 2.6 s. The plasma is in the fluctuating detachment state [10], where the impact of the high field side high density is most pronounced. This state features a detached inner divertor and an outer divertor in the high-recycling regime. The discharge is described in more details in Refs. [5, 7].

3. The Modeling Setup

The SOLPS5.0 code package [14] has been used for the modeling. SOLPS mainly consists of two coupled codes: B2.5 [15] is a fluid code that solves Braginskii-like equations for ions (D, C, He, N) and electrons. Eirene is a Monte-Carlo code that describes kinetic neutrals [16]. Both codes are coupled via source terms and are called iteratively. The reference equilibrium for the grid generation is taken at 2.4 s of the discharge #28903. The separatrix density is set by a neutral gas puff of deuterium molecules at the experimental feed-forward rate of 2.0×10^{22} e$^-$s^{-1}. A puff of nitrogen atoms at a low seeding rate ($\sim 10^{19}$ e$^-$s^{-1}) is applied to account for residual wall sources of nitrogen from seeding in the previous discharges. The densities of fully-stripped helium and carbon ions are set to fixed values at the core boundary to match the experimental core impurity concentrations. Deuterium, helium and nitrogen are assumed to be fully recycling, whereas carbon is assumed to be a sticking species. The input power into the simulation domain takes into account the core radiation – predominantly from tungsten. The latter is determined from bolometric tomography that is in accordance with power balance. The power flow across the separatrix in the simulations is 5 − 6 MW. Boundary conditions as in Ref. [7] are used with the exception of the main chamber grid boundary, where fall-off lengths of order $\lambda = 1$ cm for density and temperature profiles are used instead of loss factors. In SOLPS, the perpendicular fluxes of particles, energy and momentum are derived from ad-hoc transport coefficients. For each of these free parameters, a radial profile of χ_e, χ_i, D and $v_\perp$ is specified at the outer midplane such that a good fit of the simulations to the experimental target and midplane profile data was obtained. To mimic ballooning of transport, the transport coefficients are

Qty	Core	Pedestal	SOL
χ_e	0.1-0.5	0.05-0.2	0.1- 5.0
χ_i	0.1-0.5	0.05-0.2	0.1- 5.0
D	0.1-0.7	0.01-0.2	0.1- 2.5
$v_\perp$	0.0-0.0	0.00-5.0	0.0-70.0

Table 1 – The transport coefficients for #28903 are given. $\chi_{e,i}$ and D are in $\frac{\mathrm{m}^2}{\mathrm{s}}$ and $v_\perp$ is in $\frac{\mathrm{m}}{\mathrm{s}}$.

scaled by $\left|\frac{B_{\mathrm{ref}}}{B}\right|^2$ with a reference magnetic field $B_{\mathrm{ref}} = \frac{1}{V}\int_V B^2 dV$, where V is the volume of the modeling domain. A rescaling of the transport coefficients in the divertor volume is only used transiently during the convergence of the simulations. Identical transport coefficients are assumed for main and impurity ions. The range of transport coefficients applied can be found in Table 1. All drift terms are activated in the simulations, if not stated explicitly otherwise. The neutral model for the reactions and the atomic data is close to the one presented in Ref. [17].

4. The High Field Side High Density in SOLPS-Modeling

In the past, most power exhaust modeling of the plasma boundary – with some exceptions such as Ref. [18] – has readily discarded a substantial mismatch of the simulated inner divertor plasma with experiment. The situation was aggravated by a common lack of experimental data from the high field side scrape-off layer. However, these locations can be important in determining the boundary plasma solution in ASDEX Upgrade H-modes in the entire modeling domain. A key ingredient in how the high field side scrape-off layer plasma determines the plasma solution is the development of a high field side high density region. The inner divertor receives significantly less power (inter-ELM) than the outer divertor [19, 20], the baffling for neutrals is stronger and the parallel connection length as well as the flux expansion is larger. This leads to a colder and more dense plasma – with increased radiation losses – already for pure deuterium fueling. Strong baffling and the plasma conditions allow for a larger impurity retention

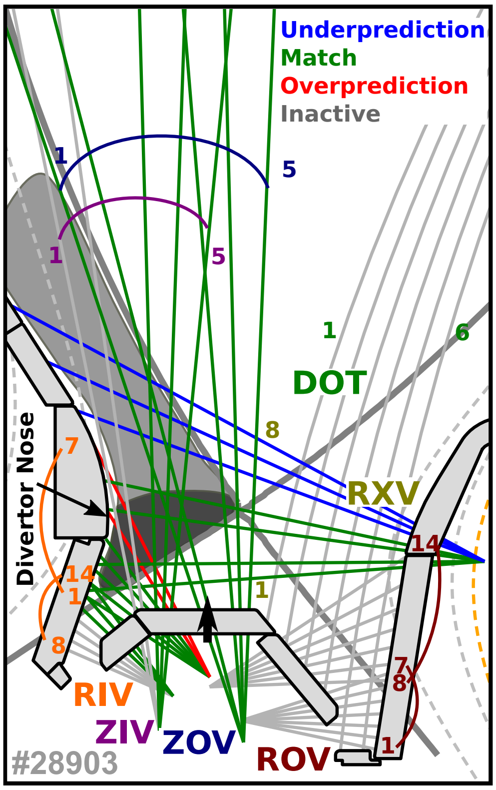

Figure 1 – The lines of sight of the divertor spectroscopy at ASDEX Upgrade are shown along with the gray shaded region of the high field side high density. The line of sight color code compares modeled and experimental densities from Stark broadening analysis.

due to a suppression of the temperature gradient force out of the divertor and an increased friction drag towards the divertor plate below the X-point. Higher impurity content in combination with high electron densities then additionally allow for increased radiation losses from low-Z impurities. These self-amplifying processes in the inner divertor lead to a transition to the high-recycling regime and to low target temperatures at lower upstream densities than for the outer divertor. As a consequence SOLPS simulations of ASDEX Upgrade usually exhibit a region of high density and low temperature ($1-2$ eV) in the inner divertor, which is initially confined to the volume between the X-point, the inner strikepoint and the divertor nose, see Figure 1. Drifts and the transport model change the spatial extent and the magnitude of this high density. The remainder of the paper will describe how the interaction of these two drivers can lead to a better match with experiment and how this allows to increase the neutral compression in the simulations.

4.1. The Role of Drifts

Activating drifts in the simulations leads to additional particle fluxes from the outer divertor into the private-flux region and from there into the inner divertor [21]. This furthers the described tendency of high density and low temperature in the inner divertor and leads to a reduction of the density and a reciprocal increase of the temperature in the outer divertor. Additional redistribution of the heat flux from the inner to the outer divertor due to drifts again amplifies the effect [22]. Lower impurity retention and lower density in the outer divertor also lead to larger in-out asymmetries of the impurity concentration and to a reduction of the radiation losses in the outer divertor. For the outer/inner target all this triggers the onset of high-recycling and detachment at higher/lower upstream densities compared to simulations without drifts. Drifts also change the particle flow pattern in the divertor and close to the X-point in the common scrape-off layer [22]. In particular on the high field side, the combination of the poloidal and perpendicular $\vec{E} \times \vec{B}$-drifts lead to additional particle fluxes into the far scrape-off layer [23]. In the drift cases we analyzed, the heat flux profile was also shifted outward into the inner far scrape-off layer. The redistributed heat and particles then help to establish a 'high-recycling' regime in the high field side far scrape-off layer by increasing the ionization sources there. The high field side high density region broadens – in perpendicular and poloidal direction – and the maximum density in the inner divertor increases. The high density region extends along the inner target to above the divertor nose and up to the inner midplane. With the increase of the recycling fluxes in the far scrape-off layer consequently the high field side neutral fluxes above the X-point are significantly increased.

A second order effect, that moderates the effect of this high-recycling in the high field side far scrape-off layer, can be exerted by the neutral conductances of the subdivertor structures of ASDEX Upgrade. These allow the high neutral fluxes of the inner divertor to migrate towards the main chamber and/or to equilibrate with the subdivertor pressure. Vice-versa high neutral subdivertor pressures can provide additional neutrals and help to sustain the high field side scrape-off layer recycling. This moderation effect can play a role in the numerical and physical stabilization of the simulations, but the neutral conductances alone in simulations without drifts so far have not been sufficient to establish high-recycling in the far scrape-off layer.

4.2. Role of Plasma Fueling

Scrutinizing the high density region in the high field side scrape-off layer, it became clear that two additional processes need to be considered for fueling of the confined plasma. Figure 2 shows density profiles at the low field side (red) and high field side (green) midplane. At the inner midplane the density gradients are in-

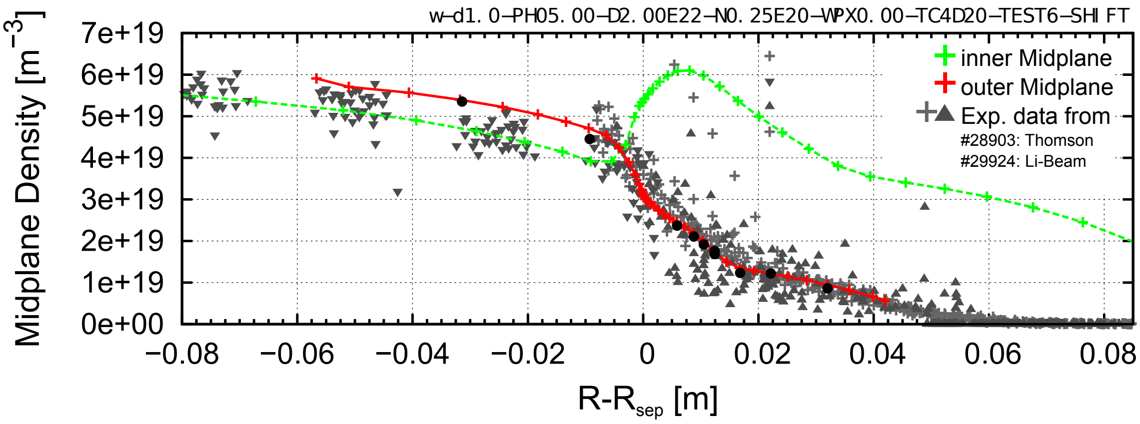

Figure 2 – The electron density profiles at the outer (red) and inner (green) midplane are shown along with experimental data at the outer midplane (grey). A clear in-out asymmetry of the scrape-off layer profiles and inverted gradients at the inner midplane separatrix can be seen.

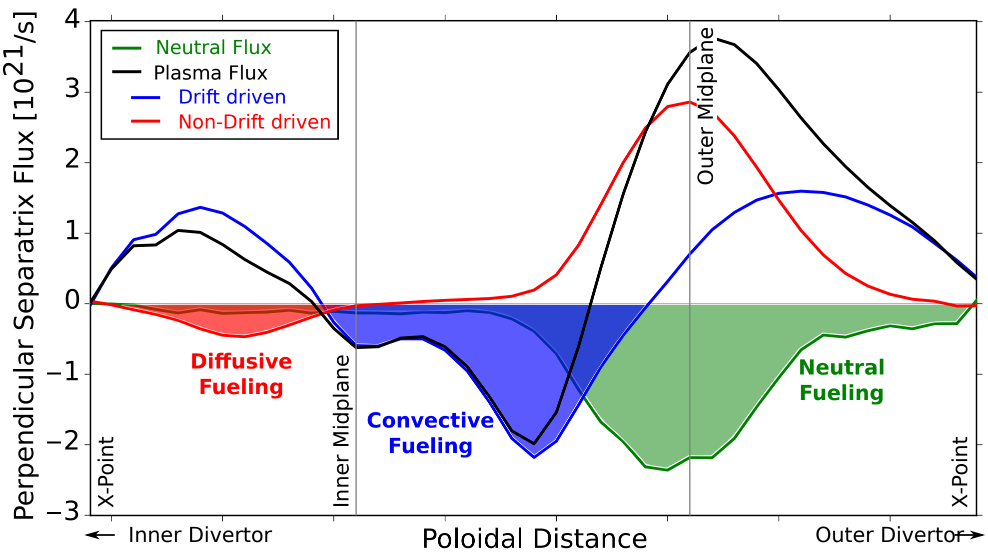

Figure 3 – The particle flux across the separatrix is plotted along the poloidal direction from X-point to X-point. The neutral fueling of the confined plasma (green) is supplemented by plasma flow driven by drifts (blue) and diffusion due to inverted density gradients (red).

verted at the separatrix. Such inverted gradients can be present in drift simulations between the X-point and the inner midplane and lead to a diffusive plasma flow across the separatrix, see red shaded region in Figure 3. In addition, a drift-driven plasma flow across the separatrix also provides a particle source for the confined plasma, see blue shaded region in Figure 3. The balance of outward and inward directed drift-driven particle flows depends on the up-down asymmetry of the plasma profiles with respect to the midplane, which is influenced by the high field side high density. The amount of particle influx can be comparable to the effective ionization source due to neutrals inside the confined plasma. Neglecting the effective particle source due to an influx of plasma into the confined region so far prohibited us to achieve the experimental neutral compression, i.e. separatrix densities *and* divertor neutral densities being simultaneously consistent with experiment. In order to achieve the correct neutral compression in the simulations, the particle diffusion coefficients need to be reduced to low values ($D \approx 0.01 - 0.05\ \frac{\mathrm{m}^2}{\mathrm{s}}$) in the proximity of the separatrix to decrease the fueling by inward diffusive plasma flow and to confine the high density more to the divertor. Including a perpendicular outward convective transport component in the low field side scrape-off layer to mimic the convective transport by filaments can further lower the fueling of the core by plasma influx. The reduction of the plasma flow into the confined plasma allows to increase the neutral fueling rates to experimental levels. A fixed pumping speed of the pumping system then automatically implies an increase of the neutral density in the divertor and in turn a significant increase of the neutral radiation. In contrast to previous modeling [7], the neutral divertor density and the neutral radiation are now also widely consistent with experimentally observed levels. The adaptation of the transport model also included a reduction of the previously necessary additional perpendicular transport in the divertor volume [7]. The reduction of the perpendicular diffusion coefficients in the divertor back to original level results in an additional increase of the gradients and the maximum of the density in the inner divertor. This has two beneficial effects with respect to an improved match to the experiment. First, the density does not extend as much out of the divertor and the density is more strongly concentrated in the vicinity of the divertor target, which further reduces the plasma influx to the confined. Second, the increase in the peak particle density leads to the onset of strong recombination, which we will discuss in the following.

4.3. The Role of Recombination

In the past, we always attempted to match the the low experimental values of the ion saturation current measurements at the inner target by locally increasing the divertor transport coefficients [7]. This paper presents that the same result can be obtained without such a rescaling of the divertor transport. Taking away the additional transport at first worsens the match to experiment. In particular, the density at and the ion fluxes to the inner divertor target increase to large values. However, with increasing density strong volumetric recombination starts to set in at the inner strikepoint and subsequently broadens along the target. It reduces the density at the inner target plate as well as the ion flux dramatically and brings the simulated target profiles back to experimental levels. The recombination sink rate is then comparable to the total recycling flux from all grid boundaries. This is a step forward in simulating ASDEX Upgrade H-modes as significant volumetric recombination had not been present in previous simulations of the fluctuating detachment state [7] in contrast to spectroscopic signatures of recombination in the inner divertor [8]. In addition, the results indicate that it might not be necessary to invoke additional physics, e.g. in Ref. [24], to reconcile modeling with experiment.

The volumetric recombination in the simulations was triggered mainly by the increase of the density in the divertor and less so by a decrease in temperatures. This indicates the importance of three-body recombination. It is yet to be evaluated to which extent increased losses (radiation, charge-exchange, ionization) due to increased neutral density in the divertor or a change in the flow pattern are important. The neutral particle source from volumetric recombination sustains the high neutral pressure in the subdivertor without the need of large recycling fluxes from the target surface, which allows for high neutral divertor pressures and low inner target ion fluxes at experimentally observed upstream separatrix electron densities. High electron density with ionizing temperatures (> 10 eV) towards the core plasma are responsible for a high opacity for neutrals towards the confined plasma. In contrast, decreasing density and temperature towards the private flux region allow the neutrals to migrate from the high density region to the subdivertor volume. Both effects combined result in high neutral subdivertor pressure and high neutral

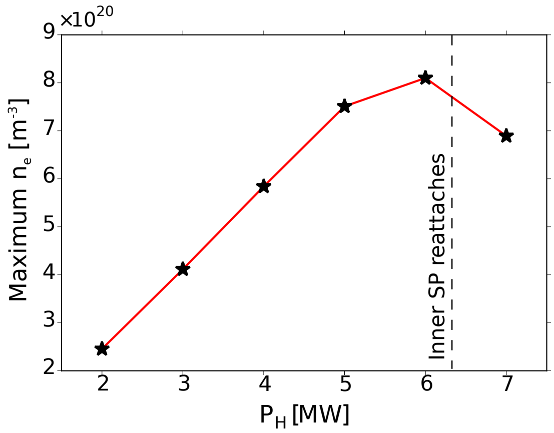

Figure 4 – Consistent with experiment, the maximum density in the high field side high density shows a linear dependence on the heating power up to a point where the inner target starts to re-attach.

compression. It is to be noted that non-drift simulations have a significantly lower peak density in the inner divertor. The high density also has a tendency to peel off the inner target and move from the divertor nose towards the X-point. A concomitant flattening of the electron density profile and a reduction of the density below the divertor nose prevents access to a state with significant recombination sinks in the inner divertor for these simulations.

4.4. The Impact of Impurity Seeding & Heating Power

Experiments have shown that the high field side high density is diminished in its spatial dimensions and its magnitude with nitrogen seeding [12]. If the nitrogen influx is increased in the simulation, the same trend is observed. First, a reduction of the density along with significantly increased radiation in the high field side scrape-off layer is observed. Concomitant with the reduction of the high field side high density a reduced influx of plasma into the confined region and hence a drop of the separatrix density is observed. This is reminiscent of experimental observations that are connected to confinement improvement with the application of nitrogen seeding [12, 13]. In the initial phase of seeding, temperatures at the outer divertor can even increase in the simulations despite the increased impurity content as the upstream density drops. The maximum target temperature then varies only slightly ($\sim$ 10%) with increased seeding until the density in the inner divertor stabilizes again. At this point the outer divertor temperature starts to drop with further increased seeding and the radiation and ionization fronts move towards the X-point to ultimately form the X-point radiation with completely detached targets. The reduction of the high field side high density with increased nitrogen seeding is accompanied by a reduction of power into the region of strong ionization as well as a reduction of the ionization source strength in the high field side scrape-off layer. This indicates that the ionization in the inner divertor is limited by the available energy for ionization and that impurity radiation leads to a power-starvation of the recycling process, i.e. the ionization source decreases due to power balance constraints [25, 26]. Simulations with a variation of the applied heating power are also in line with experimental observations and support this interpretation. Figure 4 shows a linear variation of the maximum density in the high field side high density region with the heating power up to a point where the inner strikepoint temperature starts to increase and the inner divertor starts to re-attach. The linear increase of the density with heating power is consistent with experimental evidence presented in [12]. However, in ASDEX Upgrade H-mode experiments the inner divertor is usually always detached and the roll-over of the density with re-attachment of the inner target has not been observed so far. The details of the parametric dependences and the applicable parameter ranges need to be evaluated further and in greater depth in the future.

5. Discussion & Summary

This contributions shows the importance of a decent match with experimental data from the high field side scrape-off layer in validated modeling of ASDEX Upgrade H-mode simulations. It is essential to match the low field side *and* high field side scrape-off layer and divertor plasma simultaneously. In particular, the high field side high density is an essential contributor to the overall plasma solution via the fueling of the confined plasma, the distribution of the neutral particle sources and the achievable neutral compression of the divertor. Drifts play a crucial role in forward toroidal field ($\nabla\vec{B}$-drift pointing down) in determining the spatial extent and the radial and poloidal gradients of the high field side high density. In simulations with activated drift terms, inverted radial density profiles on the high field side and drift-driven particle fluxes lead to plasma flow into the confined plasma. In the past, neglecting this plasma flow in the analysis of the fueling of the confined plasma has lead to a discrepancy of modeling and experiment in the neutral compression ratio. Adapted perpendicular diffusive transport coefficients and/or application of a convective transport component are able to reconcile the modeled neutral compression ratio with experimental values and allow to increase the divertor neutral density to experimental levels – along with neutral radiation levels, the deuterium fueling rates and the measured electron densities in the inner divertor volume. In combination with the onset of recombination in the inner divertor this allows to drop the increased perpendicular transport in the divertor that has previously been necessary in order to reduce the ion flux to the inner target.

Acknowledgements

This work has been carried out within the framework of the EUROfusion Consortium and has received funding from the Euratom research and training program 2014-2018 under grant agreement No 633053. The views and opinions expressed herein do not necessarily reflect those of the European Commission. This work has received funding under the 2015-18 EUROfusion Researcher Grants.

References

[1] M. Shimada, et al. *Nuclear Fusion*, 47(6):S1–S17, June 2007.

[2] P. Batistoni. Technical Report CCE-FU 49/6., March 2010.

[3] A. Loarte, et al. *Nuclear Fusion*, 47(6):S203–S263, June 2007.

[4] A. Kallenbach, et al. *Plasma Physics and Controlled Fusion*, 55(12):124041, December 2013.

[5] F. Reimold, et al. *Nucl. Fusion*, 55(3):033004, March 2015.

[6] M. Bernert. *Nuclear Materials and Energy*, submitted, 2016.

[7] F. Reimold, et al. *Journal of Nuclear Materials*, 463:128–134, August 2015.

[8] F. Reimold, et al. In *EPS 2015*, Lisbon, Portugal, June 2015.

[9] S. Potzel, et al. *Journal of Nuclear Materials*, 463:541–545, August 2015.

[10] S. Potzel, et al. *Nucl. Fusion*, 54(1):013001, January 2014.

[11] L. Guimarais, et al. In *EPS 2015*. European Physical Society, 2015.

[12] S. Potzel, et al. In *EPS 2015*, Lisbon, Portugal, June 2015.

[13] M. G. Dunne. In *APS 2016*, Savannah, Ohio, November 2016.

[14] R. Schneider, et al. *Contributions to Plasma Physics*, 46(1-2):3–191, February 2006.

[15] B. J. Braams. NET-Report 142/83-11/FU-NL/NET, Princeton, USA, 1987.

[16] D. Reiter, et al. *Fusion Science and Technology*, 47(2):172–186, 2005.

[17] V. Kotov, et al. *Plasma Phys. Control. Fusion*, 50(10):105012, October 2008.

[18] M. Wischmeier, et al. *Journal of Nuclear Materials*, 415(1, Supplement):S523–S529, August 2011.

[19] A. Herrmann, et al. *Plasma Phys. Control. Fusion*, 37(1):17, January 1995.

[20] A. Herrmann, et al. *Journal of Nuclear Materials*, 266–269(0):291–295, March 1999.

[21] T. D. Rognlien, et al. *Journal of Nuclear Materials*, 266–269:654–659, March 1999.

[22] L. Aho-Mantila. In *EPS 2014*, Berlin, June 2014.

[23] F. Reimold. *Experimental Studies and Modeling of Divertor Plasma Detachment in H-Mode Discharges in the ASDEX Upgrade Tokamak*. Thesis, Technical University Munich, Munich, Germany, 2015.

[24] D. Coster. *Journal of Nuclear Materials*, 415(1):S545–S548, August 2011.

[25] S. I. Krasheninnikov, et al. *Physics of Plasmas*, 4(5):1638–1646, May 1997.

[26] B. Lipschultz, et al. *Journal of Nuclear Materials*, 266–269:370–375, March 1999.